# Definition and First Application of a Probabilistic Warning Model for Rainfall-Induced Landslides

Gaetano Pecoraro and Michele Calvello

## Abstract

A methodology for the definition and the performance assessment of a probabilistic warning model for rainfall-induced landslides is proposed and tested in a study area in northern in Italy. To this aim, a database of 513 landslides triggered by rainfall in the period 2010–2018 and satellite-based rainfall data are used. It is worth mentioning that both landslide records and rainfall measurements used for this study are open-access datasets available online. The methodology developed herein can be summarized into several successive steps. First, an automated algorithm is applied for reconstructing the rainfall conditions responsible for the documented landslides in the area of analysis, as well as the rainfall conditions that did not result in any landslide. Then, the conditional probabilities of landslide occurrence are calculated using a two-dimensional Bayesian analysis, differentiating between single landslide events (SLE) and areal landslide events (ALE). Subsequently, several thresholds at different conditional probabilities are evaluated, and different combinations are selected for the activation of two warning levels. For each rainfall combination, the issuing of warning levels is computed by comparing the conditional probability of landslide occurrence with the pre-defined warning level thresholds. Finally, the optimal thresholds combination to be employed, i.e. the one providing the best model performance in terms of success and error indicators, is selected using performance indicators derived from a 3 by 3 contingency table.

## Introduction

Rainfall-induced landslides are widespread and destructive natural phenomena occurring all around the world that often cause severe human and economic losses (Froude and Petley 2018). Landslide early warning systems (LEWS) are being increasingly applied as non-structural risk mitigation measures. LEWS can be designed and employed at two different reference scales (Calvello 2017; Pecoraro et al. 2019): local systems address single landslides at slope scale (Lo-LEWS), while territorial systems (Te-LEWS) deal with multiple landslides over wide areas at regional.

Te-LEWS are used to provide generalized warnings over appropriately-defined homogeneous warning zones of relevant extension. Typically, these systems address weather-induced landslides through the monitoring and prediction of meteorological parameters. However, the definition of a regional warning model may be challenging for several reasons: the reconstruction of rainfall events, the absence of a direct relationship between rainfall and landslide initiation, the uncertainty of available landslide catalogues (e.g., Piciullo et al. 2018; Segoni et al. 2018a).

In this study, a conceptual framework for the definition of probabilistic rainfall thresholds for landslides at regional scale is developed. The main steps of the proposed approach are: (i) objective reconstruction of triggering and non-triggering rainfall conditions taking into account their frequency, (ii) probabilistic analysis, (iii) definition and performance evaluation of a two-levels probabilistic warning model. The proposed procedure has been tested by analyzing the reported landslides in the period 2010–2018 within a study area in northern Italy.

G. Pecoraro (✉) · M. Calvello
Department of Civil Engineering (DICIV), University of Salerno, Via Giovanni Paolo II, 132, 84084 Fisciano, (SA), Italy
e-mail: gpecoraro@unisa.it

M. Calvello
e-mail: mcalvello@unisa.it

## Materials and Methods

### Study Area and Database

The study area includes 6 of the 158 weather warning zones (*WZ*) defined for hydrogeological risk management in Italy: *Emil-E*, *Emil-G*, *Ligu-B*, *Ligu-C*, *Tosc-L*, and *Tosc-S1* (Fig. 1). Although the selected *WZ* fall into three different Italian regions, all of them are characterized by high susceptibility to the occurrence of rainfall-induced landslides.

Indeed, the study area is one of the rainiest of Italy; moreover, climate change is producing an extraordinary increase of rainfall intensity in there (Libertino et al. 2018). As a consequence, this area is one of the most severely affected by landslides in the last few years in Italy (Battistini et al. 2013).

In particular, thunderstorms characterized by intense and very intense rainfall cause widespread and damaging ground effects, both on the slopes and along the drainage pattern, in *Ligu-B*, *Ligu-C*, *Tosc-L*, and *Tosc-S1* (Roccati et al. 2018). Besides, the frequency of rapid shallow landslides is markedly increasing in the last few years in *Emil-E* and *Emil-G*, as shortest and more intense rainfalls, typically the main triggering factor of shallow landslides and debris flows in the Emilia-Romagna region, became more frequent in the Mediterranean area due to climate change (Segoni et al. 2018b).

The FraneItalia database (Calvello and Pecoraro 2018) reports 540 landslide events that occurred in the study area in the period 2010–2018. 27 records have been excluded from the analysis performed herein as they are reported as human- or earthquake-induced landslides or landslides for which the trigger is not known. Among the 513 landslide events included in the dataset, 353 are classified as single landslide events (SLE, red circles in Fig. 1) and the remaining 160 as areal landslide events (ALE, blue squares in Fig. 1).

The rainfall measurements were derived from the satellite-based Tropical Rainfall Measuring Mission (TRMM) database, which is a joint mission between NASA and the Japan Aerospace Exploration Agency (JAXA) launched in late November 1997 for the study of rainfall for weather and climate research purposes (Huffmann et al. 2007). Precipitation data used in this research have been derived from the TRMM version 3b42, which includes gridded precipitation data collected every 3 h at a $0.25° \times 0.25°$ ($\sim 25$ km $\times$ 25 km) spatial resolution, extending from latitude 50° S to latitude 50° N. It is worth mentioning that the spatial resolution is finer respect to local rain gauge networks usually employed for early warning purposes.

Satellite rainfall data retrieved from TRMM database have been analyzed using Google Earth Engine (https://earthengine.google.com), a cloud-based platform for planetary-scale environmental data analysis. For the purposes of this study, precipitation measurements have been aggregated at 3-hourly temporal resolution and the mean rainfall values over each territorial unit have been calculated.



**Fig. 1** Shaded relief map of the study area showing the 540 rainfall-induced "FraneItalia" landslide records in the period 2010–2018, differentiated in single (red circles) and areal landslide events (blue squares). The inset shows the location of the six warning zones in Italy
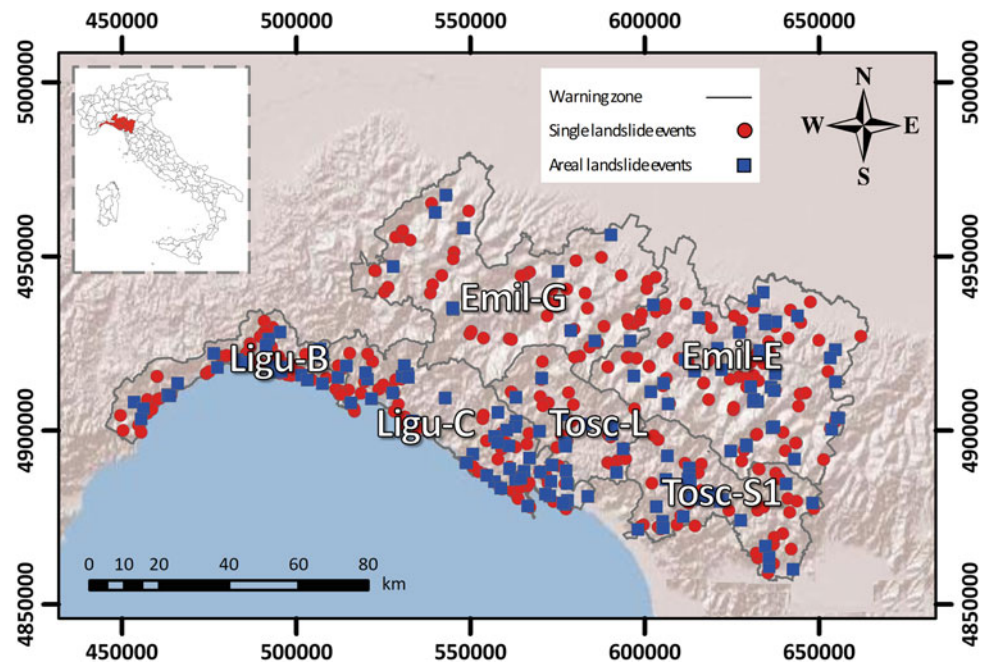
## Methodology

The methodology developed for the definition of the probabilistic thresholds of landslides occurrence can be schematized into three main phases: reconstruction of the rainfall events, probabilistic analysis and definition of the probabilistic warning model.

In the first phase, the correlation between landslides and rainfall events in the study area is conducted by reconstructing the rainfall events, in order to convert a series of hyetographs into a point cloud in a graph reporting triggering and non-triggering combinations of rainfall parameters. Duration ($D$) and cumulated rainfall ($E$) are identified as the most appropriate rainfall parameters to use. To this aim, a modified version of the "algorithmic" approach developed by Melillo et al. (2016) is applied.

A reduced set of parameters to account for different physical settings and operational conditions has been considered. In particular, all the parameters are differentiated considering the "warm" springer-summer period, $C_W$, and the "cold" autumn–winter period, $C_C$ (Table 1).

The automated procedure is based on several steps. In the pre-processing step ($S_0$), the rainfall records lower than a predefined threshold $GS$ are considered noise and are set to $E_H = 0.0$ mm. The remaining steps are differentiated into two main logical blocks. The first block performs the automatic reconstruction of the rainfall events and can be schematized in the following four steps: ($S_1$) detection of the isolated rainfall events considering a dry interval, $R_1$ and exclusion of irrelevant events that do not exceed a predefined threshold $E_R$; ($S_2$) identification of rainfall sub-events proceeded and followed by dry periods with no rain, $R_2$; ($S_3$) exclusion of irrelevant sub-events, whose cumulated (total) rainfall, $E_S$ is lower than a given threshold, $R_3$; ($S_4$) identification of rainfall events, constituted either by a period of continuous rainfall or by an ensemble of periods considering a minimum dry period, $R_4$. Successively, in the second block the algorithm combines information on temporal occurrence of rainfall events and landslide events, performing three additional steps: ($S_5$) selection of triggering and non-triggering rainfall events; ($S_6$) reconstruction of multiple aggregations of rainfall sub-events that are likely to trigger landslides; ($S_7$) reconstruction of multiple aggregations of rainfall sub-events that did not trigger landslides. All the triggering and non-triggering sub-events identified by the algorithm are equally possible.

In the second phase, a probabilistic approach based on a two-dimensional Bayesian analysis, similar to that used by Berti et al. (2012), is developed to calculate the landslide probability associated to the different rainfall combinations. To this aim, the posterior landslide probability is evaluated considering the joint probability of the duration ($D$) and cumulated rainfall ($E$), as follows:

$$P(L|D,E) = \frac{P(L) \times P(D,E|L)}{P(D,E)} \tag{1}$$

where: $P(L|D, E)$ is the posterior landslide probability; $P(L)$ is the prior probability; $P(D, E|L)$ is the likelihood; $P(D, E)$ is the marginal probability. The needed probabilities have been determined considering that the triggering and non-triggering rainfall conditions are expressed in terms of multiple combinations, as follows:

$$P(L) = \frac{N_L}{N_R} \tag{2}$$

$$P(D,E) = \frac{\sum_i n_{i,(D,E)} \times f_i}{N_R} \tag{3}$$

$$P(D,E|L) = \frac{\sum_i n_{i,(D,E|L)} \times f_i}{N_L} \tag{4}$$

where: $N_L$ is the total number of landslide events that occurred in the period of analysis; $N_R$ is the total number of rainfall events recorded in the period of analysis; $n_{i,(D,E)}$ is the number of possible rainfall conditions characterized by specific values of $D$ and $E$; $n_{i,(D,E|L)}$ is the number of rainfall events characterized by specific values of $D$ and $E$ that resulted in landslides; $f_i$ is the relative frequency, defined as

Table 1 Parameters used for the application of the algorithm developed by Melillo et al. (2016)

| Step | Parameter name | Parameter value | | Unit |
|------|----------------|-------|-------|------|
| | | $C_W$ | $C_C$ | |
| $S_0$ | GS | 0.2 | 0.2 | mm |
| $S_1$ | $E_R$ | 0.2 | 0.2 | mm |
| $S_1$ | $R_1$ | 3 | 6 | h |
| $S_2$ | $R_2$ | 6 | 12 | h |
| $S_3$ | $R_3$ | 1 | 1 | mm |
| $S_4$ | $R_4$ | 48 | 96 | h |

**Table 2** Warning levels defined considering the probabilities of SLE and ALE

| Warning level | Correlation law |
|---|---|
| WL$_1$ | P(L\|D, E)$_{SLE}$ > P$_1$ |
| WL$_2$ | P(L\|D, E)$_{SLE}$ > P$_2$ or P(L\|D, E)$_{ALE}$ > P$_1$ |



**Fig. 2** Contingency matrix used for the performance analysis of the probabilistic rainfall thresholds

the inverse of the total number of possible aggregations of sub-events for a given rainfall event.

In the third phase, a warning model is defined employing two warning levels (WL$_1$ and WL$_2$) associated to the exceedance of two thresholds (P$_1$ and P$_2$) based on the probabilities of occurrence of SLE and ALE (Table 2).

In the fourth phase, the performance of the warning model is analyzed using statistical indicators, following a procedure similar to that proposed by Calvello and Piciullo (2016). In particular, the performance analysis of a 3 by 3 contingency matrix is based on a set of two performance criteria, both of them assigning a meaning to all the elements of the matrix (Fig. 2). The "alert classification" criterion employs an alert classification scheme derived from a standard 2 by 2 contingency table, and identifies correct predictions (CP), false alerts (FA), missed alerts (MA), and true negatives (TN). The "grade of accuracy" criterion assigns a colour code to the components of the matrix in relation to the agreement between a given warning event and a given landslide event. Using this criterion, the elements are classified in four colour-coded classes, as follows: green (Gre) for the elements which are assumed to be representative of

the best model response, yellow (Yel) for elements representative of minor model errors, red (Ora) for elements representative of a significant model error and purple (Red) for elements representative of a severe model error.

Considering the two performance criteria, several performance indicators can be derived. Table 3 lists the indicators used in this study.

## Results

### Rainfall Events Reconstruction

1903 rainfall conditions (D, E) have been identified and plotted in log–log coordinates (Fig. 3). The 207 rainfall conditions responsible for triggering 353 SLE (red circles in Fig. 3) and the 129 rainfall conditions responsible for 160 ALE (blue squares in Fig. 3) are in the range of duration $3 \leq D \leq 915$ h and in the range of cumulated rainfall $1.02 \leq E \leq 243.54$ mm. The non-triggering rainfall conditions, reconstructed in the same period, are 1567 (green circles in Fig. 3). They are in the ranges of $3 \leq D \leq 495$ h and $1.01 \leq E \leq 311.87$ mm.

It is worth mentioning that rainfall combinations characterized by $E < 2$ mm (grey circles in Fig. 3) constitute a negligible amount of rain, thus these combinations have been excluded from the analysis because they are considered irrelevant for the purpose of early warning.

### Probabilistic Analysis

The definition of the probabilistic thresholds is based on a two-dimensional Bayesian analysis evaluating the conditional probability of landslide occurrence given the joint probability of D and E. According to the available data, the

**Table 3** Performance indicators used for the performance analysis

| Performance indicator | Symbol | Formula |
|---|---|---|
| Efficiency index | I$_{eff}$ | (TN + CP)/Σ$_{ij}$d$_{ij}$ |
| Odds ratio | OR | (TN + CP)/(FA + MA) |
| Probability of serious mistakes | P$_{SM}$ | Red/Σ$_{ij}$d$_{ij}$ |
| Probability of serious missed alerts | P$_{SM-MA}$ | MA$_{Red}$/MA |
| Probability of serious false alerts | P$_{SM-FA}$ | FA$_{Red}$/FA |
| Missed and false alert balance | MFB | MA/(MA + FA) |
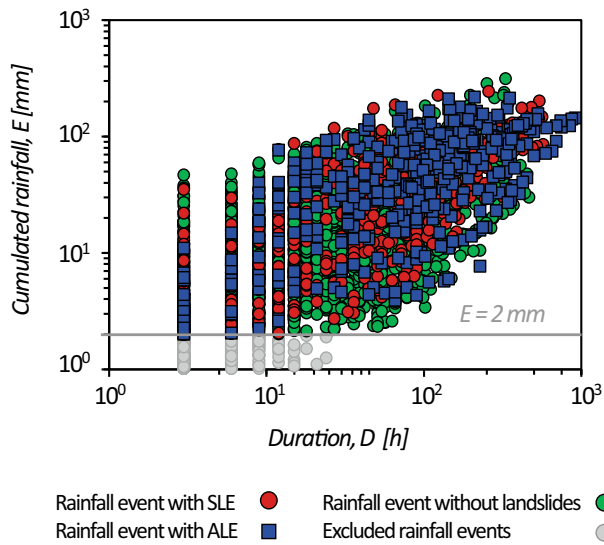
**Fig. 3** Rainfall duration (D) versus cumulated rainfall (E) in the study area from 2010 to 2018. Graph plotted in log–log coordinates



**Fig. 4** Posterior landslide probabilities obtained considering SLE (**a**) and ALE (**b**)
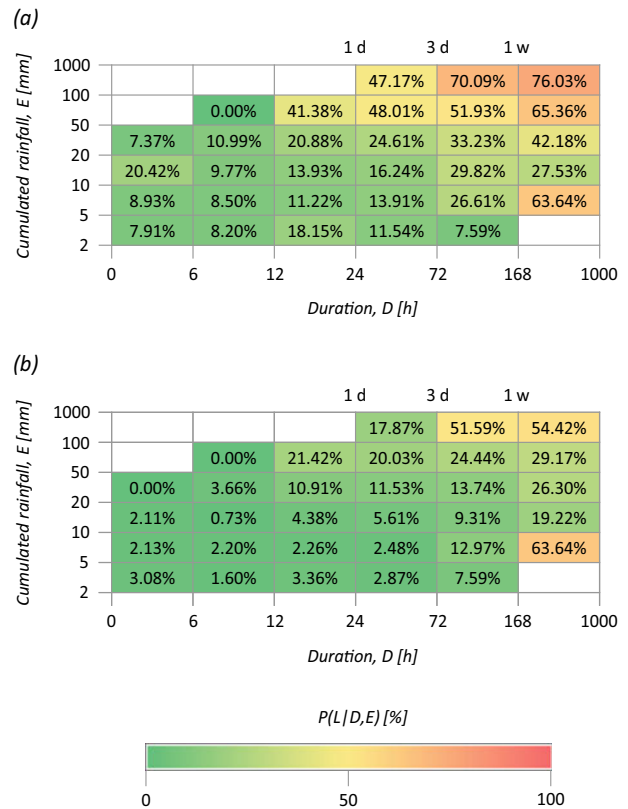
prior landslide probability, $P(L)$ has been calculated using Eq. (2) and is equal to 18.79% for SLE and 7.44% for ALE.

Successively, the $D$, $E$ space reported in Fig. 3 has been divided in $6 \times 6$ cells, both for SLE and ALE, and the posterior landslide probabilities, $P(L|D, E)$, have been calculated by applying Eq. (1). Looking at SLE, Fig. 4a displays that long-duration ($12 \leq D \leq 915$ h), high-accumulation rainfall ($50 \leq E \leq 243.54$ mm) events show the highest landslide probabilities ($P(L|D, E) > 40\%$). The only singularity is represented by the combination $5 \leq D \leq 10$ h, $50 \leq E \leq 243.54$ mm, for which $P(L|D, E) = 63.64\%$. However, this can be considered a singularity, as it represents only 0.02% of the rainfall combinations that occurred from 2010 to 2018. The results are substantially confirmed for ALE (Fig. 4b). Indeed, apart for the singularity already highlighted for SLE, the highest values of the posterior probability ($P(L|D, E) > 20\%$) are reached again for $12 \leq D \leq 915$ h and $50 \leq E \leq 243.54$ mm.

## Probabilistic Warning Model

A performance evaluation has been conducted in order to identify the optimal two thresholds to be employed in the warning model. Several combinations have been compared, by varying the lower threshold, $P_1$ and the upper threshold, $P_2$. As significant differences in the performance evaluation depend only on the variations of $P_1$, the results are reported grouping the thresholds on the basis of $P_1$ (Table 4).

Table 5 shows the results obtained for the five combinations considering the elements of the correlation matrix

reported in Fig. 2. Higher values of $CP$ and $Yel$ are obtained when the lower probabilities values are considered to define $WL_1$ ($P_1$ from 10 to 20%). In particular, passing from $P_{20,40–50}$ to $P_{30,50}$ results in a reduction of $CP$ of about 37%. However, an increase of the $P1$ threshold results in a significant reduction of the $FA$ and $Red$ errors and increasing values of $TN$.

Table 6 shows the results in terms of success ($I_{eff}$ and $OR$) and error ($P_{SM}$, $P_{SM-MA}$, $P_{SM-FA}$, and $MFB$) indicators for the five different thresholds combinations reported in Table 4. Concerning the success indicators and, in particular, the efficiency index ($I_{eff}$), raising the value of $P_1$, a general increase is observed, as it is evident when comparing $P_{10,20–50}$ and $P_{12.5,25–50}$ to $P_{20,40–50}$ and $P_{30,50}$. The odds ratio ($OR$), which can be considered a rate between correct and wrong predictions, obviously increases with the reduction of $FA$ and the increment of $TN$. However, it should be noted that passing from $P_{20,40–50}$ to $P_{30,50}$ the Probability of serious missed alerts ($P_{SM-MA}$) shows an increment of about 25%. Besides, the majority of the errors are missed alerts, as demonstrated by the high value of $MFB$ (60.72%). For these reasons, $P_{20,40–50}$ can be considered the best-performing thresholds combination of the 5 considered herein.

**Table 4** Combinations considered to identify the optimal values of P₁ and P₂

| Label | P$_1$ (%) | P$_2$ (%) |
|---|---|---|
| P$_{10,20-50}$ | 10 | 20, 25, 30, 40, 50 |
| P$_{12.5,25-50}$ | 12.5 | 25, 30, 40, 50 |
| P$_{15,30-50}$ | 15 | 30, 40, 50 |
| P$_{20,40-50}$ | 20 | 40, 50 |
| P$_{30,50}$ | 30 | 50 |

**Table 5** Number of contingency matrix elements considering the "alert classification" (CP, TN, MA, FA) and "grade of accuracy" (Gre, Yel, Ora, Red) criteria

| Element | P$_{10,20-50}$ | P$_{12.5,25-50}$ | P$_{15,30-50}$ | P$_{20,40-50}$ | P$_{30,50}$ |
|---|---|---|---|---|---|
| CP | 249.87 | 233.66 | 209.51 | 185.24 | 115.85 |
| TN | 564.59 | 692.42 | 841.70 | 960.76 | 1183.58 |
| MA | 51.80 | 68.01 | 92.15 | 116.42 | 185.81 |
| FA | 739.21 | 611.38 | 462.09 | 343.04 | 120.21 |
| Gre | 701.24 | 821.86 | 956.25 | 1060.83 | 1248.63 |
| Yel | 113.22 | 104.21 | 94.96 | 85.17 | 50.81 |
| Ora | 434.78 | 509.22 | 408.42 | 346.81 | 207.70 |
| Red | 356.22 | 170.16 | 145.83 | 112.65 | 98.32 |

**Table 6** Performance indicators computed for the five thresholds combinations considered

| Indicator | P$_{10,20-50}$ | P$_{12.5,25-50}$ | P$_{15,30-50}$ | P$_{20,40-50}$ | P$_{30,50}$ |
|---|---|---|---|---|---|
| I$_{eff}$ | 50.73% | 57.68% | 65.48% | 71.38% | 80.94% |
| OR | 1.03 | 1.36 | 1.90 | 2.49 | 4.25 |
| P$_{SM}$ | 19.92% | 9.50% | 6.72% | 6.66% | 6.12% |
| P$_{SM-MA}$ | 25.46% | 25.16% | 25.43% | 26.03% | 32.91% |
| P$_{SM-FA}$ | 41.48% | 22.16% | 18.29% | 22.35% | 30.92% |
| MFB | 6.55% | 10.01% | 16.63% | 25.34% | 60.72% |

## Conclusions

In this study, a Bayesian approach has been developed for the definition of a probabilistic warning model for rainfall-induced landslides. It has been defined using a landslide inventory retrieved from online news and satellite-based rainfall measurements. Both landslide records and satellite rainfall monitoring used in this study come from open-access datasets available online.

Firstly, the triggering and non-triggering rainfall conditions have been objectively reconstructed. Then, a Bayesian approach has been applied for calculating the posterior landslide probabilities of occurrence of single landslide events (SLE) and areal landslide events (ALE). Finally, a probabilistic warning model employing two thresholds has been defined and its performance evaluated using performance indicators derived from a 3 by 3 contingency table.

The performed analyses showed that P$_{20,40-50}$ is the best-performing thresholds combination, as it represents the best compromise between the minimization of incorrect landslide predictions and the maximization of the correct predictions. Generally, the probabilistic warning model revealed an overall good performance in predicting landslide events triggered by significantly different rainfall conditions. Although the performance of the model can be further refined considering wider and longer datasets, the preliminary results achieved herein clearly allow to highlight its potential for landslide early warning purposes.

## References

Battistini A, Segoni S, Manzo G, Catani F, Casagli N (2013) Web data mining for automatic inventory of geohazards at national scale. Appl Geogr 43:147–158

Berti M, Martina MLV, Franceschini S, Pignone S, Simoni A, Pizziolo M (2012) Probabilistic rainfall thresholds for landslide occurrence using a Bayesian approach. J Geophys Res 117:F04006

Calvello M (2017) Early warning strategies to cope with landslide risk. Riv It Geotecnica 2:63–91

Calvello M, Pecoraro G (2018) FraneItalia: a catalog of recent Italian landslides. Geoenviron Disasters 5(13).

Calvello M, Piciullo L (2016) Assessing the performance of regional landslide early warning models: the EDuMaP method. Nat Hazards Earth Syst Sci 16:103–122

Froude MJ, Petley DN (2018) Global fatal landslide occurrence from 2004 to 2016. Nat Hazards Earth Syst Sci 18:2161–2181

Huffman GJ, Adler RF, Bolvin DT, Gu G, Nelkin EJ, Bowman KP, Hong Y, Stocker EF, Wolff DB (2007) The TRMM multi-satellite precipitation analysis: quasi-global, multi-year, combined-sensor precipitation estimates at fine scale. J Hydrom 8(1):38–55

Libertino A, Ganora D, Claps P (2018) Space-time analysis of rainfall extremes in Italy: clues from a reconciled dataset. Hydrol Earth Syst Sci 22(5)

Melillo M, Brunetti MT, Peruccacci S, Gariano SL, Guzzetti F (2016) Rainfall thresholds for the possible landslide occurrence in Sicily (southern Italy) based on the automatic reconstruction of rainfall events. Landslides 13(1):165–172

Pecoraro G, Calvello M, Piciullo L (2019) Monitoring strategies for local landslide early warning systems. Landslides 16:213–231

Piciullo L, Calvello M, Cepeda JM (2018) Territorial early warning systems for rainfall induced landslides. Earth Sci Rev 179:228–247

Roccati A, Faccini F, Luino F, Turconi L, Guzzetti F (2018) Rainnfall events with shallow landslides in the Entella catchment (Liguria, northern Italy). Nat Hazards Earth Syst Sci 18:2367–2386

Segoni S, Piciullo L, Gariano SL (2018a) A review of the recent literature on rainfall thresholds for landslide occurrence. Landslides 15:1483–1501

Segoni S, Rosi A, Fanti R, Gallucci A, Monni A, Casagli N (2018b) A regional-scale landslide warning system based on 20 years of operational experience. Water 10(10):1297